Received: 24 November 2022 | Revised: 7 March 2023 | Accepted: 9 March 2023

DOI: 10.1111/cts.13517

ARTICLE

Population pharmacokinetics, enzyme occupancy, and 24*S*-hydroxycholesterol modeling of soticlestat, a novel cholesterol 24-hydroxylase inhibitor, in healthy adults

Wei Yin[1] | **Axel Facius**[2] | **Thomas Wagner**[2] | **Max Tsai**[3] | **Mahnaz Asgharnejad**[1] | **Gëzim Lahu**[2] | **Majid Vakilynejad**[1]

[1]Takeda Pharmaceutical Company Ltd., Cambridge, Massachusetts, USA

[2]thinkQ[2] AG, Baar, Switzerland

[3]Takeda Development Center Americas Inc., Deerfield, Illinois, USA

Correspondence
Majid Vakilynejad, Takeda Pharmaceuticals, 40 Landsdowne Street, Cambridge, MA 02139, USA.
Email: majid.vakilynejad@takeda.com

Abstract

Soticlestat is a first-in-class, selective inhibitor of cholesterol 24-hydroxylase (CH24H), which catabolizes cholesterol to 24*S*-hydroxycholesterol (24HC) in the brain, in phase III development for Dravet syndrome and Lennox–Gastaut syndrome treatment. This study aimed to develop a model of soticlestat pharmacokinetics (PKs) and pharmacodynamics (PDs) using 24HC plasma concentrations and CH24H enzyme occupancy (EO) time profiles. Subsequently, model-based simulations were conducted to identify dosing strategies for phase II trials in children and adults with developmental and epileptic encephalopathies (DEEs). Four phase I trials of healthy adults involving oral administration of soticlestat 15–1350 mg were used to develop the mixed-effect population PK/EO/PD model. The population PK analysis utilized 1727 observations (104 individuals), PK/EO analysis utilized 20 observations (11 individuals), and PK/PD analysis utilized 2270 observations (99 individuals). Optimal dosing strategies were identified from model-based PK, EO, and PD simulations. The PK/EO/PD model described the observed data well and comprised a two-compartment model with dose as a covariate on peripheral volume, linear elimination, and intercompartmental clearance. Transit and effect-site compartments were included to accommodate different dosage forms and the delay between plasma drug concentrations and EO. Model-based simulations indicated that soticlestat 100–300 mg twice daily may be an optimal adult dosing regimen with weight-adjusted pediatric dosing strategies identified for evaluation in phase II trials. The population PK/EO/PD model provided understanding of the soticlestat PK/PD relationship with partial delineation of sources of variability, and identified dosing strategies for phase II trials of children and adults with DEEs.

Study Highlights

WHAT IS THE CURRENT KNOWLEDGE ON THE TOPIC?

Soticlestat, a selective inhibitor of cholesterol 24-hydroxylase (CH24H), is in phase III development for the treatment of Dravet syndrome and Lennox–Gastaut syndrome.

WHAT QUESTION DID THIS STUDY ADDRESS?

What are the pharmacokinetic (PK) and pharmacodynamic (PD) profiles of soticlestat in healthy adults, and what dosing strategies are suggested using model-based simulations for phase II clinical trials in pediatric and adult patient populations?

WHAT DOES THIS STUDY ADD TO OUR KNOWLEDGE?

The developed population mixed-effect model of soticlestat adequately described the observed data from healthy adults in terms of PKs, enzyme occupancy, and PDs. Soticlestat 300 mg twice daily was identified as the optimal dosing strategy to explore in phase II clinical trials in adults with developmental and epileptic encephalopathies (DEEs). Model-based simulations of the exposure–response relationship were used to recommend specific weight-adjusted doses, which were explored in phase II clinical trials in children and adolescents with DEEs weighing under 60 kg.

HOW MIGHT THIS CHANGE CLINICAL PHARMACOLOGY OR TRANSLATIONAL SCIENCE?

These findings illustrate the utility of model-based simulations to select dosing strategies for clinical trials. This model-based approach expedites the drug development process by allowing direct development from healthy adults to pediatric patient populations, which is vital for rare and severe pediatric conditions such as DEEs.

INTRODUCTION

Soticlestat is a first-in-class, selective inhibitor of cholesterol 24-hydroxylase (CH24H; also known as CYP46A1) that is currently in phase III development for the treatment of the developmental and epileptic encephalopathies (DEEs) Dravet syndrome (DS) and Lennox–Gastaut syndrome (LGS). CH24H is the primary enzyme responsible for the catabolism of cholesterol to 24*S*-hydroxycholesterol (24HC) in the brain.[1–3] Given that aberrant cholesterol metabolism often occurs in neurological disorders that involve seizures (e.g., DS and LGS), inhibition of CH24H may have therapeutic relevance in these disorders.[4,5] Model-informed drug development (MIDD) can be an indispensable tool for rare conditions, such as DS and LGS, to aid dose selection and study design optimization. This approach is also particularly useful for facilitating clinical development of new drugs in pediatric populations.[6,7]

Soticlestat has been shown to bind specifically to CH24H and to reduce brain 24HC levels in preclinical studies.[1,8] In an in vitro enzyme assay, soticlestat inhibited the activity of human CH24H in a concentration–dependent manner with a half-maximal inhibitor concentration (IC_{50}) of 4.5 nmol/L.[1] In wild-type mice, single oral administration of soticlestat dose-dependently reduced 24HC levels in the brain, with a statistically significant reduction seen 24 h after administration of 3 mg/kg and 10 mg/kg doses (25% and 33% reductions in 24HC levels, respectively, vs. controls).[8] Furthermore, a positron emission tomography (PET) study in nonhuman primates showed that soticlestat bound specifically to brain CH24H, with 100% occupancy observed after administration of soticlestat 0.89 mg/kg.[9]

Further preclinical evaluation of the relationship of soticlestat pharmacokinetics (PKs), pharmacodynamics (PDs), and target enzyme occupancy (EO) led to the definition of target CH24H occupancy threshold for efficacy of at least 65%. Subcutaneous administration of soticlestat 1, 3, and 10 mg/kg in a pentylenetetrazol-induced kindling mouse model dose-dependently suppressed seizure progression, with the 1 mg/kg dose resulting in an ~60% reduction of mean brain 24HC levels and an estimated average EO close to 65%.[10] Based on preclinical data, a two-compartment model with Michaelis–Menten type elimination was developed that described observed PK and PD preclinical data and accounted for the observed nonlinear properties of soticlestat (unpublished data). Together, these findings supported investigation of soticlestat in clinical settings.[1]

In a first-in-human single-rising-dose study, soticlestat 15–1350 mg was rapidly absorbed after oral solution administration, with a median time to maximum plasma

concentration (T_{max}) of 0.25–0.52 h. The mean maximum plasma concentration (C_{max}) and area under the plasma concentration–time curve from zero to infinity (AUC_{∞}) increased more than dose-proportionally, by 183-fold and 581-fold, respectively. Mean terminal elimination half-life ($t_{½z}$) also varied across the dose range, from 4.4 to 7.2 h for soticlestat 200–1350 mg (the 15 mg and 50 mg doses had limited quantifiable concentration data during the terminal phase). No apparent difference was observed in mean plasma 24HC concentrations between the placebo and soticlestat 15 mg groups, although mean plasma 24HC concentrations were numerically lower in the soticlestat 50–1350 mg groups. Maximum reductions in 24HC levels were observed ~16 h after dosing in the 50, 200, and 600 mg groups, and ~48 h after dosing in the 900 mg and 1350 mg groups.[11]

Findings were similar in a multiple-rising-dose study of healthy adults receiving an oral solution of soticlestat 100–600 mg once daily (q.d.) or 300 mg twice daily (b.i.d.) for 10–14 days. C_{max} was reached rapidly, with a median T_{max} of 0.3–0.5 h, and mean $t_{½z}$ was ~4 h. Over the six-fold dose range, mean soticlestat C_{max} and AUC_{∞} on day 1 increased 6.55-fold and 9.35-fold, respectively. Dose-dependent decreases in plasma 24HC concentrations were observed over the 14 days, with maximum reduction by day 7. Soticlestat 100–400 mg q.d. reduced 24HC levels by 46.8%–62.7% on day 14 based on the AUC 0 to 24 h ($AUC_{0\text{-}24h}$).[12] Additionally, C_{max} was shown to be lower when participants were fasting and receiving soticlestat 300 mg as a tablet formulation than when they were receiving the equivalent dose as an oral solution or receiving a tablet in a fed state. Exposure measured as AUC_{∞} was similar between the different administrations.[11]

In healthy adults receiving single doses of soticlestat 50–600 mg, PET imaging with the [^{18}F]MNI-792 ligand demonstrated that soticlestat crossed into the brain and blocked the tracer from binding to the enzyme target. Global EO was calculated based on total brain volume of distribution of tracer, and measured occupancy was both dose- and time-dependent. Occupancy increased with increasing dose and ranged from 11% (50 mg dose at 24 h) to 96% (600 mg dose at 2 h). Soticlestat elimination was slower from brain tissue than from plasma based on occupancy measurements at 10 and 24 h.[13,14]

In an absolute bioavailability and mass balance study in healthy male volunteers, soticlestat was almost completely absorbed with an absolute bioavailability of 12.6% after administration of a single 300 mg dose. These findings suggest that a substantial amount of soticlestat undergoes first-pass metabolism. Additionally, soticlestat was found to be rapidly metabolized with the main pathway involving direct glucuronidation on the hydroxyl group of soticlestat to form M3. This pathway was mediated by uridine 5′-diphospho-glucuronosyltransferase (UGT) 1A9 and UGT2B4, with the latter being the predominant metabolizing enzyme. All other metabolic pathways were demonstrated to be minor, including oxidation mediated by cytochrome P450 (CYP) 3A4 or CYP2C19, and oxidation followed by glucuronidation. M3, the glucuronide conjugate of soticlestat, was therefore the major circulating metabolite and the major elimination pathway of soticlestat.[15] Furthermore, soticlestat was demonstrated to be a weak substrate of P-glycoprotein and was not a substrate of breast cancer resistance protein, organic anion transporting polypeptide (OATP) 1B1, or OATP1B3.

Here, we describe the use of MIDD for soticlestat to expedite the translation of dosing strategies from healthy adults to children with DEEs. The key aim of the present analysis was to develop a mixed-effect population model of soticlestat PK and PD, using 24HC plasma concentrations and EO data from healthy adults. The second aim was to carry out simulations to inform dose selection and study design for optimal safety and efficacy in phase II studies involving adults and children with DEEs.

A mixed-effect population PK (PopPK) model of soticlestat was developed and sequentially linked to an EO/PD model to describe the relationship between soticlestat PK, EO (brain CH24H occupancy based on a PET imaging study) and PD (plasma 24HC profiles). Subsequently, model-informed simulations were conducted to guide soticlestat dose selection and study design for a phase Ib/IIa clinical trial evaluating safety and tolerability in adults with DEEs,[4] and a phase II clinical trial evaluating safety and efficacy in children with DS or LGS.[7]

METHODS

Study population and data collection

Data from healthy adults in four phase I studies were used to develop the PK/EO/PD model (Table 1): a single-rising-dose study, a multiple-rising-dose study, an open-label PET study, and a bioavailability and food effect study.[11–13] Soticlestat was administered as an oral solution in all studies, except the food effect study in which both oral solution and tablet formulations were used. Demographic and individual characteristics data were collected at baseline across the studies, including age, race, sex, and body mass index (BMI).

Plasma soticlestat concentrations were measured by high-performance liquid chromatography with tandem mass spectrometry (HPLC–MS/MS). The assay was validated with a concentration range from 1.00 ng/mL (lower limit of quantitation [LLOQ]) to 2000 ng/mL. Plasma 24HC levels were measured by HPLC–MS/MS within a validated concentration range from 2.00 ng/mL (LLOQ) to 100 ng/mL.[11,12] Sampling schedules are summarized in Table 1.

TABLE 1 Overview of completed phase I studies upon which the model was based.

ClinicalTrials.gov and study identifiers	Objectives	Design and population	Dosing information	Sampling schedule
NCT02201056 TAK-935_101[11]	To evaluate safety, tolerability, PK, and PD	Randomized, double-blind, placebo-controlled single-rising-dose study 48 healthy male and female participants, 19–55 years of age	Soticlestat 15, 50, 200, 600, 900, and 1350 mg, single dose, oral solution, fasted condition	Plasma soticlestat concentrations: 4 mL blood samples collected on day 1, <0.5 h before dosing, and at 0.25, 0.5, 1, 1.5, 2, 3, 4, 6, 8, 10, 12, 16, 24, 36, 48, 72, and 96 h after dosing. Plasma 24HC concentrations: 8 mL blood samples collected on days −1 and 1, <0.5 h before dosing, and at 0.5, 1, 2, 4, 6, 8, 12, and 16 h after dosing.
NCT02539134 TAK-935-1002[12]	To evaluate safety, tolerability, PK, and PD	Randomized, double-blind, placebo-controlled multiple-rising-dose study 40 healthy male and female participants, 18–55 years of age	Soticlestat 100, 300, 400, and 600 mg q.d. and 300 mg b.i.d., for 10 days or 14 days, oral solution, fasted condition	Plasma soticlestat concentrations: 4 mL blood samples collected <0.5 h before dosing and at 0.17, 0.25, 0.33, 0.5, 1, 1.5, 2, 3, 4, 6, 8, 10, 12, 16, and 24 h after dosing on day 1 and day 14, with trough sampling <0.5 h before dosing on days 7, 11, 12, and 13. Additional blood samples were collected on day 7 for the 400 mg q.d. cohort at 0.25, 0.5, 1, 2, 4, and 8 h after dosing. Plasma 24HC concentrations: 8 mL blood samples collected before dosing and at 0.5, 1, 2, 4, 8, 12, 16, and 24 h after dosing on days −1, 1, and 14. Additional trough samples were taken <0.5 h before dosing on days 7, 12, and 13. For patients who received b.i.d. dosing, blood samples were collected up to 12 h after morning dosing.
NCT02497235 TAK-935-1003[13]	To evaluate brain CH24H occupancy using the PET ligand [^{18}F]MNI-792 and PET imaging, and the relationship between occupancy and exposure	Nonrandomized, open-label PET study 11 healthy male participants, 19–55 years of age	Soticlestat 50, 100, 200, 300, or 600 mg, single dose, oral solution, fasted condition [^{18}F]MNI-792, i.v., ≤370 MBq (≤10 mCi), single dose/PET scan	Plasma soticlestat concentrations: blood samples collected at three timepoints after dosing (just after tracer injection [for PET scan imaging], 1 h after tracer injection, and 2 h after tracer injection). Plasma 24HC concentrations: blood samples collected on day −1 at 1, 4, and 12 h after check; on day 1, ≤0.5 h before dosing; and at 1, 4, 8, 12, 20, 24, and 30 h after dosing.
NCT02906813 TAK-935-1005[11]	To evaluate relative bioavailability of soticlestat in tablet versus solution formulation, and the effect of food	Randomized, open-label, three-way crossover single-dose study 9 healthy male and female participants, 18–55 years of age	Soticlestat 300 mg (as three 100 mg tablets), single oral dose, fed or fasted condition, or soticlestat 300 mg (solution), single oral dose, fasted condition	Plasma soticlestat concentrations: 4 mL blood samples collected <0.5 h before dosing and at 0.17, 0.25, 0.33, 0.5, 1, 1.5, 2, 3, 4, 6, 8, 10, 12, 16, 24, 36, and 48 h after dosing on day 1 in each dosing period.

Abbreviations: 24HC, 24*S*-hydroxycholesterol; b.i.d., twice daily; CH24H, cholesterol 24-hydroxylase; i.v., intravenous; MBq, megabecquerel; mCi, millicurie; PD, pharmacodynamics; PET, positron emission tomography; PK, pharmacokinetics; q.d., once daily.

In the PET imaging study, brain CH24H occupancy was measured using the PET ligand [^{18}F]MNI-792 administered intravenously at dose levels up to 370 megabecquerel.[13] Participants underwent dynamic PET imaging scans performed once at baseline and twice following soticlestat dosing, with the post-dose scans occurring either both on the day of soticlestat dosing, or one on the day of dosing and one on the following day. The PET imaging data were analyzed with Logan graphical analysis, fixing linear regression equilibration time to 30 min using the metabolite-corrected arterial plasma input function, to calculate the total distribution volume (V_T). Global occupancy was estimated directly using V_T from the slope of the occupancy plots:

$$V_T(\text{baseline}) - V_T(\text{after dosing}) = \text{occupancy} \cdot \left(V_T[\text{baseline}] - V_{\text{ND}}\right)$$

V_{ND} is the nondisplaceable volume of distribution.

Although the extent of CH24H occupancy was expected to affect both brain and plasma 24HC concentrations, only plasma 24HC concentrations were measured.

All studies were conducted in accordance with International Council for Harmonization Good Clinical Practice guidelines, applicable local regulations, and the ethical principles that have their origin in the Declaration of Helsinki. All the participants gave written informed consent prior to participation in the studies.[11,12]

Model development

Initial development of the PopPK model for soticlestat plasma concentrations was based on graphical exploration of the data. Several standard structural models, as well as random variability error terms (both between and within individuals), were investigated.

Subsequently, CH24H occupancy data were included in the analysis data set and a direct link model characterizing the sigmoidal relationship between soticlestat concentrations and CH24H occupancy in the brain was characterized (PK/EO model).

As a third step, plasma 24HC concentrations were included in the analysis data set and their relationship with soticlestat concentrations was characterized using an indirect link turnover model (PK/PD model; Figure 1).

Data

All available data were used from the four studies, comprising 1727 observations from 104 individuals for the initial PopPK model, 20 observations from 11 individuals for the PK/EO model, and 2270 observations from 99 individuals for the PK/PD model. No data were excluded or imputed.

Software

The nonlinear mixed effects models were developed using NONMEM version 7.3 and 7.4 (ICON Development Solutions, Ellicott City, MD). Data processing and graph development were carried out with R version 3.2 or higher (R Core Team, Vienna, Austria).

Model assessment and comparison

The most appropriate model was selected based on evaluation of several initial structural models that were assessed against prespecified criteria, including those for goodness-of-fit (GOF). Each model was assessed based on individual and population parameter estimates and their precision (relative standard error), numerical convergence properties, biological plausibility, diagnostic and GOF plots, and objective function values based on the likelihood of the model fit for nested models and Akaike's or Bayesian information criterion for non-nested models. Base and final models were qualified using prediction-corrected visual predictive checks (with 1000 model-based simulations), which provide a simulation-based method to visually assess concordance of the model-based simulations and observed data. In addition, model stability was evaluated using standard nonparametric bootstrap with replacement ($n = 1000$) analysis.

Covariate model development

No formal covariate screening was performed; however, selected variables including dose (to characterize nonlinearities) and weight (to support allometric scaling of parameters) were tested as covariates on parameters with interindividual variability (IIV) components.

Clinical trial simulations

Clinical trial simulations were performed to identify suitable dosing strategies with the tablet formulation of soticlestat for phase II studies in adults and children with DEEs. These model-based simulations assessed PK, EO, and PD profiles across various scenarios, including q.d. compared with b.i.d. dosing and weight-adjusted dosing (based on allometric principles), to identify dosing

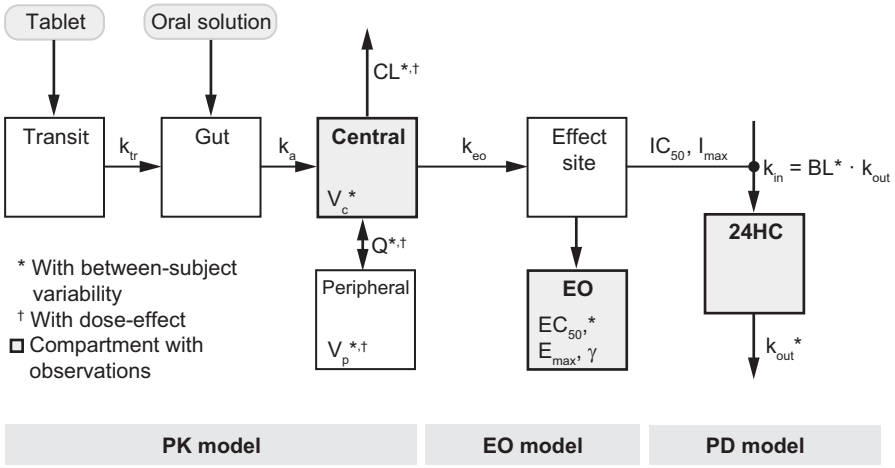

FIGURE 1 Schematic illustration of the PK/EO/PD (24HC) model. 24HC, 24*S*-hydroxycholesterol; BL, baseline 24HC; CL, oral clearance; EC_{50}, effect-site concentration required for 50% maximum effect; E_{max}, maximum effect; EO, enzyme occupancy; γ, shape parameter; IC_{50}, effect-site concentration required for 50% I_{max}; I_{max}, maximal inhibition of 24HC production; k_a, absorption rate; k_{eo}, delay rate; k_{in}, 24HC generation rate; k_{out}, 24HC degradation rate; k_{tr}, transfer rate for tablets; PD, pharmacodynamics; PK, pharmacokinetics; Q, intercompartmental apparent clearance; V_c, volume of distribution of the central compartment; V_p, apparent volume of distribution for the peripheral compartment.

strategies that would achieve similar exposures and corresponding PD responses to those seen in previous healthy adult studies. The likelihood of dosing regimens achieving a meaningful anti-seizure response in patients was assessed with two criteria: whether the dosing regimen achieved reasonable CH24H occupancy, and whether the dosing regimen achieved maximal PD response in terms of the 24HC exposure–response relationship.

Based on preclinical data, CH24H occupancy greater than 65% throughout the day was defined as the target threshold for efficacy (unpublished data). No differences in maturation stage were expected because the target population was at least 2 years of age. Target expression levels in the brain were assumed to be consistent across the selected age range, and the production and disposition of 24HC was assumed to be comparable between children and adult populations.

Model-based simulation analyses evaluated q.d. compared with b.i.d. dosing regimens and examined exposure–response relationships at different dose levels based on CH24H occupancy and 24HC levels. Soticlestat concentrations, CH24H occupancy, and change from baseline 24HC levels were simulated during 21 days of dosing followed by a 7-day washout period for a typical healthy adult (70 kg weight) receiving soticlestat at either 100 mg b.i.d., 200 mg b.i.d., or 300 mg b.i.d., or the equivalent q.d. doses (200 mg, 400 mg, and 600 mg, respectively).

Further model-based simulations were performed to investigate potential pediatric doses for investigation in clinical trials. The model was extended using weight-based allometric scaling components. The extent of exposure (AUC at steady state [AUC_{ss}] and C_{max}) and CH24H occupancy were simulated for soticlestat tablets administered 20–300 mg b.i.d. (in 20 mg increments) within various weight groups (10–60 kg in 5 kg increments). For each weight group and dose level, 500 simulations were carried out. Median and 90% prediction intervals for AUC_{ss} were calculated and compared with a reference patient weighing 70 kg who was treated with a soticlestat 100 mg (low), 200 mg (middle), or 300 mg (high) b.i.d. dosing regimen, which were used to define low, middle, and high dose recommendations for each weight group. Above 60 kg, the low, middle, and high reference doses were 100, 200, and 300 mg b.i.d., respectively. The initial dose selection was based on individual weights in 1 kg increments to identify the minimal feasible dose with a median pediatric exposure at or above the median adult reference exposure. The following rule for selecting each dose level was utilized:

$$\text{median } AUC_{ss}(\text{simulated}) \geq \text{median } AUC_{ss}(\text{reference})$$

For feasible application in a clinical trial setting, dose recommendations were summarized in weight bins with 5 kg increments. The results were visualized by plotting the simulated AUC_{ss}, CH24H occupancy, and change from baseline 24HC per weight bin with the appropriate reference values.

RESULTS

Study population and demographics

There were 9–48 healthy adults per study with a mean (standard deviation [SD]) age of 34.7 (9.6) years and mean

(SD) BMI of 25.6 (2.9) kg/m^2. Most participants were men (69%, $n = 74$) and of White ethnic background (72%, $n = 78$; Table S1).

PopPK model

A two-compartment model with first-order absorption and elimination described the observed data well. No intravenous data were used for the model development; therefore, the absolute bioavailability (F) could not be estimated. To accommodate different dosage forms, a transit compartment was included in the model, which allowed characterization of the delay in absorption for the tablet formulation (Figure 1). Observed nonlinearity in PK parameters was addressed by including dose as a covariate on oral clearance (CL/F), intercompartmental apparent clearance (Q/F), and apparent volume of distribution for the peripheral compartment (V_p/F). Weight was not tested as a covariate because of the limited range in the analysis data set; however, weight was added to the model prior to the pediatric simulations using power functions with weight centered at 70 kg.

$$\frac{\mathrm{CL}}{F} = \left(\frac{\mathrm{Dose}}{300}\right)^{-0.278} \cdot \left(\frac{\mathrm{Weight}}{70}\right)^{0.75} \cdot 204 \left[\frac{\mathrm{L}}{\mathrm{h}}\right],$$

$$\frac{V_c}{F} = 65.5 \cdot \left(\frac{\mathrm{Weight}}{70}\right)^{-1} [\mathrm{L}]$$

The parameter estimates and their relative standard errors are presented in Table 2, including estimates of IIV for transfer rate, CL/F, Q/F, volume of distribution of the central compartment (V_c/F), and V_p/F. The typical clearance (at a dose of 300 mg) was estimated at 204 L/h with a coefficient of variation (CV) of 36%. Because of the identified nonlinearity, clearance was estimated to be higher with lower doses (e.g., 277 L/h at 100 mg). The V_c/F was estimated at 65.5 L with a CV of 61%. GOF plots (Figure S1) and visual predictive checks (Figure 2) demonstrated that the model was appropriate, and bias and precision were reasonable based on the bootstrap analysis (Table 2). The NONMEM control stream for the final model is in Appendix S1. The differential equations describing the PopPK model are in Appendix S2.

PK/EO model

Changes in brain CH24H occupancy values were noticeably delayed after changes in plasma drug concentration (C_{central}), based on modeling of PopPK model-predicted plasma soticlestat concentrations and brain occupancy values. To account for this, an effect-site compartment was included in the PK/EO model, directly linking the predicted soticlestat concentrations at the effect site (C_{effect}) with brain EO values using a sigmoidal maximal EO (E_{max}) model.

$$\frac{\mathrm{d}}{\mathrm{d}t} C_{\mathrm{effect}} = \left(C_{\mathrm{central}} - C_{\mathrm{effect}}\right)$$

$$EO = \frac{\mathrm{E}_{\mathrm{max}} \cdot C_{\mathrm{effect}}^{\gamma}}{\mathrm{EC}_{50}^{\gamma} + C_{\mathrm{effect}}^{\gamma}}$$

Bias and precision were reasonable based on the bootstrap analysis (Table 2). GOF plots and visual predictive checks are shown in Figure S2.

PK/PD model

The PK/PD model was developed by fixing EO model parameters to estimates obtained in the PK/EO modeling step. As such, model-predicted soticlestat C_{effect} values were linked with 24HC plasma concentrations (C_{24HC}) using a semimechanistic inhibitory indirect response model.

$$\frac{\mathrm{d}C_{\mathrm{24HC}}}{\mathrm{d}t} = k_{\mathrm{in}} \cdot \left(1 - \frac{\mathrm{I}_{\mathrm{max}} \cdot C_{\mathrm{effect}}^{\gamma}}{\mathrm{IC}_{50} + C_{\mathrm{effect}}^{\gamma}}\right) - k_{\mathrm{out}} \cdot C_{\mathrm{24HC}}$$

The IIV for each structural PK/EO/PD parameter was evaluated, when possible, using an exponential error model.

$$X_j = \widetilde{X}_j \cdot e^{\left(\eta_j^x\right)}$$

In which, X_j = the true value of the X parameter in the jth subject; $\widetilde{X}_j$ = the population mean value of the X parameter in the jth subject; η_j^x = intersubject variability: the difference between the true and the population mean value of the X parameter in the jth subject; the η_j^x are independent, identically distributed random variables with a mean of 0 and a variance equal to ω^2.

Residual errors for PK, EO, and PD were modeled using a mixed additive and proportional error model.

$$c_{i,j} = \hat{c}_{i,j} + \varepsilon_{i,j}$$

In which: $c_{i,j}$ is the ith observation from the jth subject; $\hat{c}_{i,j}$ is the individual model prediction for that observation; $\varepsilon_{i,j}$ are independent, identically distributed random variables with a mean of 0 and a variance $w^2 = w_a^2 + \left(\hat{c}_{i,j} \bullet w_{\mathrm{p}}\right)^2$, in which w_a is the additive component and w_p is the proportional component of the variance w^2.

TABLE 2 Population PK, PK/EO and PK/PD (24HC) model parameter estimates and precision

		Original		Bootstrap			
Parameter	**Role**	**Estimate**	**RSE (%)**	**Mean**	**RSE (%)**	**95% CI**	**Bias (%)[a]**
Population PK model							
Residual variability	Proportional (%)	45.4	983	45.3	2.81	42.9, 47.9	−0.287
	Additive (ng/mL)	0.001	Fixed	0.001			0
Absorption rate (k_a)	TV (L/h)	2.13	28.7	2.14	2.93	2.02, 2.28	0.69
	BSV	0	Fixed	0			
Oral clearance (CL/F)[b]	TV (L/h)	204	1231	203	4.75	185, 223	−0.0393
	Dose effect (exponent)	−0.278	3598	−0.283	17.4	−0.381, −0.194	1.99
	BSV	0.353	1534	0.347	21.9	0.075, 0.177	−3.49
Volume of distribution of the central compartment (V_c/F)[b]	TV (L)	65.5	496	66.1	8.79	55.3, 78.1	0.922
	BSV	0.562	2874	0.563	29.8	0.157, 0.526	0.329
Intercompartmental apparent clearance (Q/F)[b]	TV (L/h)	52.6	138	52.1	8.77	44, 61.9	−0.884
	Dose effect (exponent)	−0.554	461	−0.552	12.7	−0.684, −0.408	−0.427
	BSV	0.418	238	0.415	40.7	0.0548, 0.319	−1.74
Apparent volume of distribution for the peripheral compartment (V_p/F)[b]	TV (L)	356	44.8	353	11.1	281, 433	−0.797
	Dose effect (exponent)	−0.684	80.9	−0.658	16.5	−0.852, −0.44	−3.7
	BSV	0.616	389	0.624	31.2	0.187, 0.656	2.87
Transit rate for tablets (k_{tr})	TV (L/h)	2.47	28.4	2.51	15.1	1.83, 3.33	1.37
	BSV	0.981	480	0.976	30.6	0.458, 1.56	−1.09
EO (PK/EO) model							
Residual variability	Proportional (%)	0	Fixed	0			
	Additive (ng/mL)	2.88	16.5	2.58	24.6	1.2, 3.67	−10.6
Delay rate (k_{EO})	TV (L/h)	0.255	14	0.265	56.6	0.148, 0.381	3.98
Maximum EO (E_{max})	TV (%)	100	Fixed	100			0
Effect-site concentration for 50% maximum effect (EC_{50})	TV (ng/mL)	5.86	21.6	5.93	24.3	2.88, 8.47	1.12
	BSV	0.692	62.6	0.647	32.5	0.113, 0.661	−12.5
Shape parameter (γ)	TV	0.769	9.15	0.784	14.2	0.606, 1.09	1.95
24HC (PK/PD) model							
Residual variability	Proportional (%)	0.001	Fixed	0.001			0
	Additive (ng/mL)	3.4	0.00454	3.4	3.77	3.15, 3.66	−0.0385
Baseline 24HC (BL_{24HC})	TV (ng/mL)	45.9	0.0151	46	2.28	44, 48.2	0.285
	BSV	0.474	65.1	0.472	5.33	0.199, 0.245	−0.837
24HC degradation rate (k_{out})	TV (1/h)	0.0182	3.04	0.0187	7.92	0.0157, 0.0214	3.13
	BSV	0.631	4.42	0.589	29.1	0.178, 0.548	−12.9
Effect-site concentration for 50% maximum effect (IC_{50})	TV (ng/mL)	5.21	0.00601	5.49	26.9	3.2, 9.11	5.32
Maximum 24HC inhibition (I_{max})	TV (%)	78.2	3.09	77.8	4.57	70.9, 85.1	−0.532

Abbreviations: 24HC, 24*S*-hydroxycholesterol; BSV, between subject variability (original estimate and bootstrap mean on approximate standard deviation scale, bootstrap RSE and 95% CI on variance scale); CI, confidence interval; EO, enzyme occupancy; PD, pharmacodynamic; PK, pharmacokinetic, RSE, relative standard error; TV, typical value.

[a]Bias refers to the percentage difference between the bootstrap mean and original estimate.

[b]Estimated after oral administration ("/F").

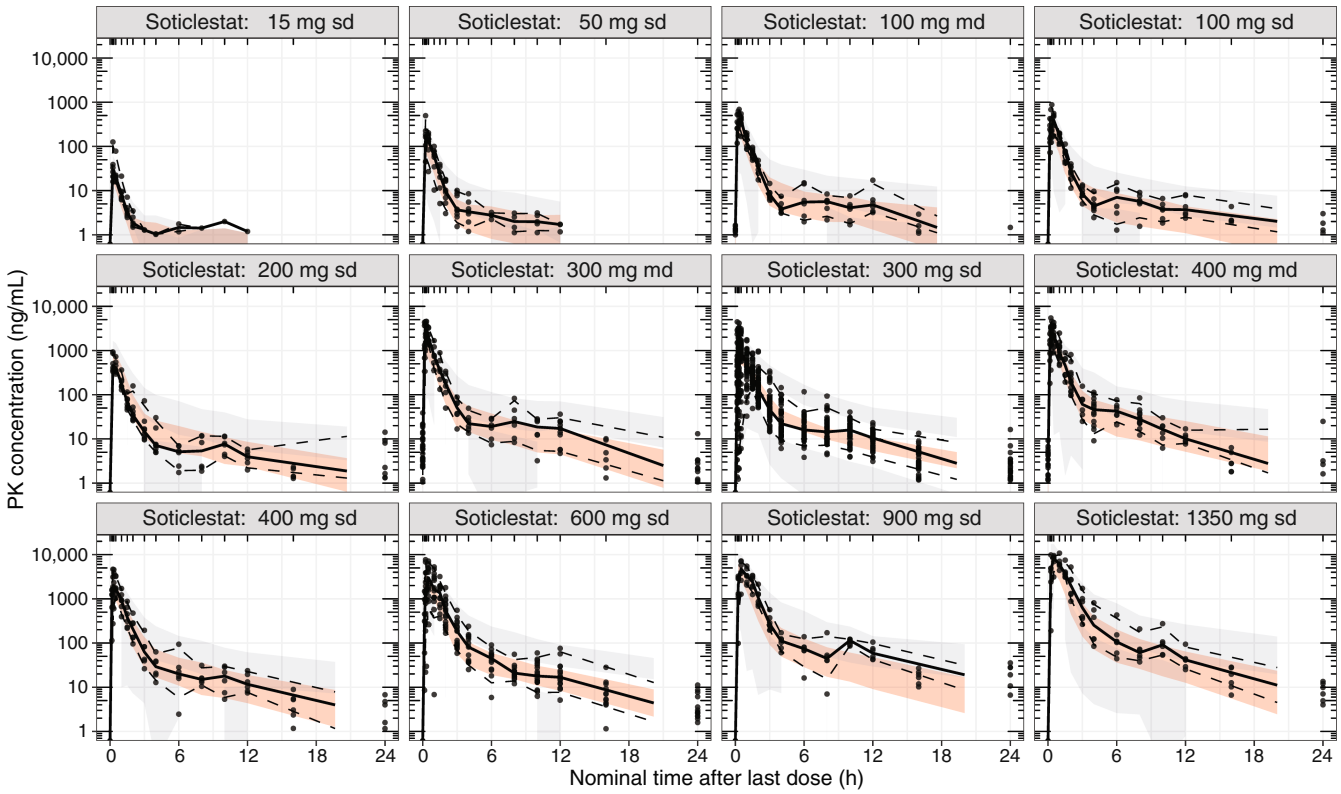

FIGURE 2 Visual predictive checks for the population PK model stratified by dose level. md, multiple dose; PK, pharmacokinetic; sd, single dose.

For the PK model, the additive component w_a was fixed at 0.001 and w_p was estimated, for the PK/EO model, w_a was estimated and w_p was fixed at 0, and for the PK/PD model, w_a was estimated and w_p was fixed at 0.001.

The resulting model described the data well and parameters were generally estimated with good precision. Bias and precision were both reasonable based on the bootstrap analysis (Table 2). GOF plots and visual predictive checks by grouped dose level are shown in Figure 3, with visual predictive checks for all individual dose levels provided in Figure S3.

Based on the model, the mean percent change in plasma 24HC from baseline to day 21 was −73.4% with soticlestat 300 mg b.i.d.

Clinical trial simulations

The PK/EO/PD model was used to simulate soticlestat concentration–time, CH24H occupancy, and 24HC concentration–time profiles at steady-state following oral administration of soticlestat 20–600 mg b.i.d. or 200–600 q.d. for 21 days. These simulations were conducted to guide dose selection for subsequent clinical studies in adults and children with DEEs. The simulated age and body weight ranges for pediatric patient populations were 2–17 years and 10–60 kg, respectively. Age-appropriate weight bins and other relevant characteristics were selected for the simulations to match predefined demographics in planned clinical studies, and height and weight charts from the Centers for Disease Control and Prevention.[16]

In simulations for an adult weighing 70 kg, b.i.d. dosing was associated with a greater proportion of time above the target CH24H occupancy of 65% and with lower fluctuations during the dosing interval than q.d. dosing. These findings were consistent for each dosage level (300 mg b.i.d. vs. 600 mg q.d. shown in Figure 4). All b.i.d. doses (100–300 mg) had desired PK/EO/PD profiles, with 300 mg b.i.d. achieving the highest CH24H occupancy levels (Figure 4).

Further simulations involved assessment of weight-based dosing strategies for children with weights up to 60 kg, by evaluating PK, EO, and PD profiles against a reference adult receiving 100 mg (low), 200 mg (middle), or 300 mg (high) soticlestat b.i.d. Within the low and middle dose levels, a small number of the simulated exposures were 30% above the reference values for a 70 kg patient (Table S2); for the high dose, the AUC_{ss} for the lower weight groups were more than 20% higher than the respective reference median AUC_{ss} (Tables S2 and S3). To avoid significantly higher exposures than the reference value, the recommended high dose for the 10–14 kg weight group

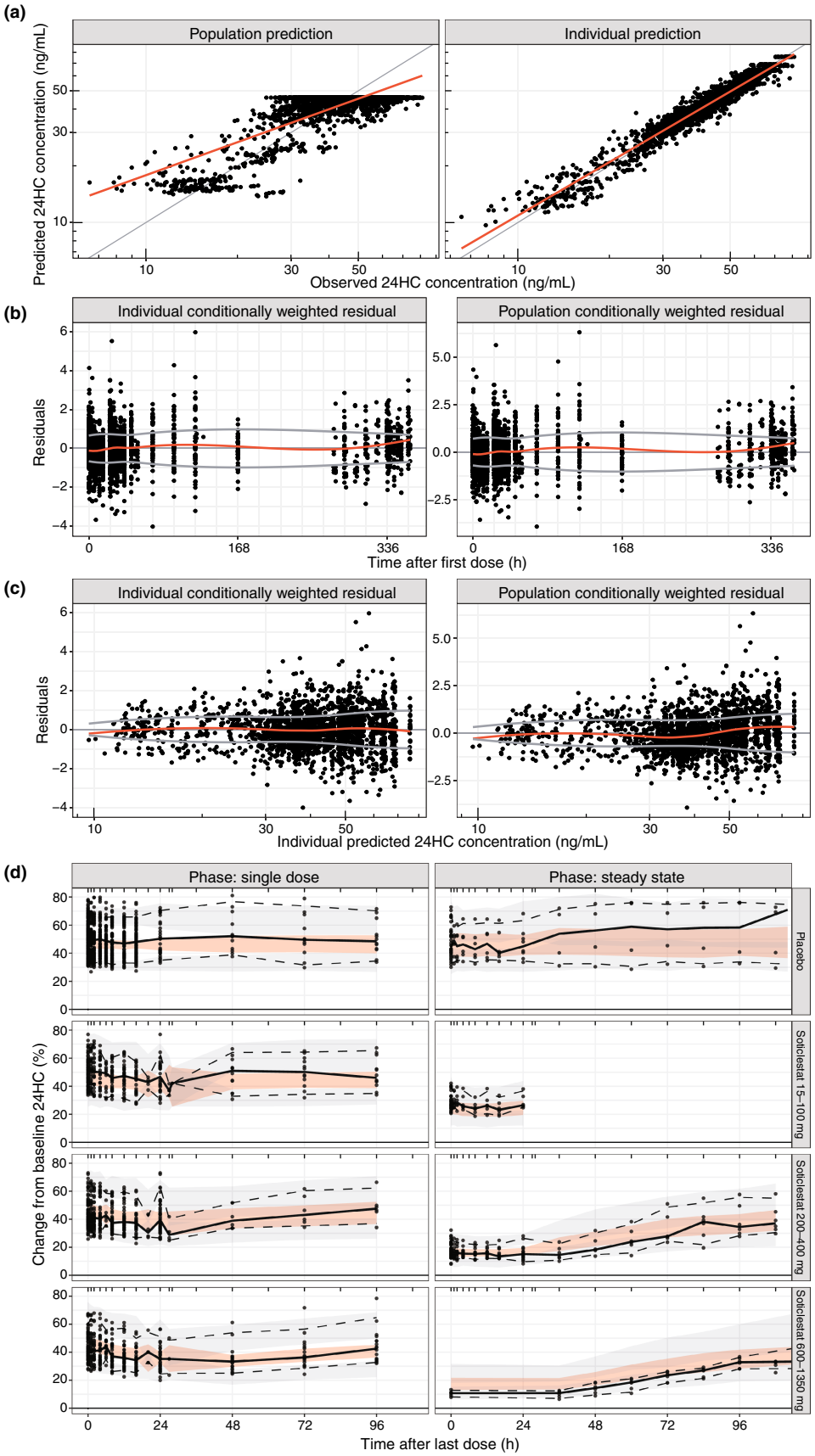

FIGURE 3 Goodness-of-fit and visual predictive checks for the PK/PD (24HC) model. (a) Predicted versus observed 24HC concentrations, (b) residuals versus time after first dose, (c) residuals versus individual predicted 24HC concentrations, (d) visual predictive checks stratified by grouped dose level. 24HC, 24*S*-hydroxycholesterol; PD, pharmacodynamic; PK, pharmacokinetic.

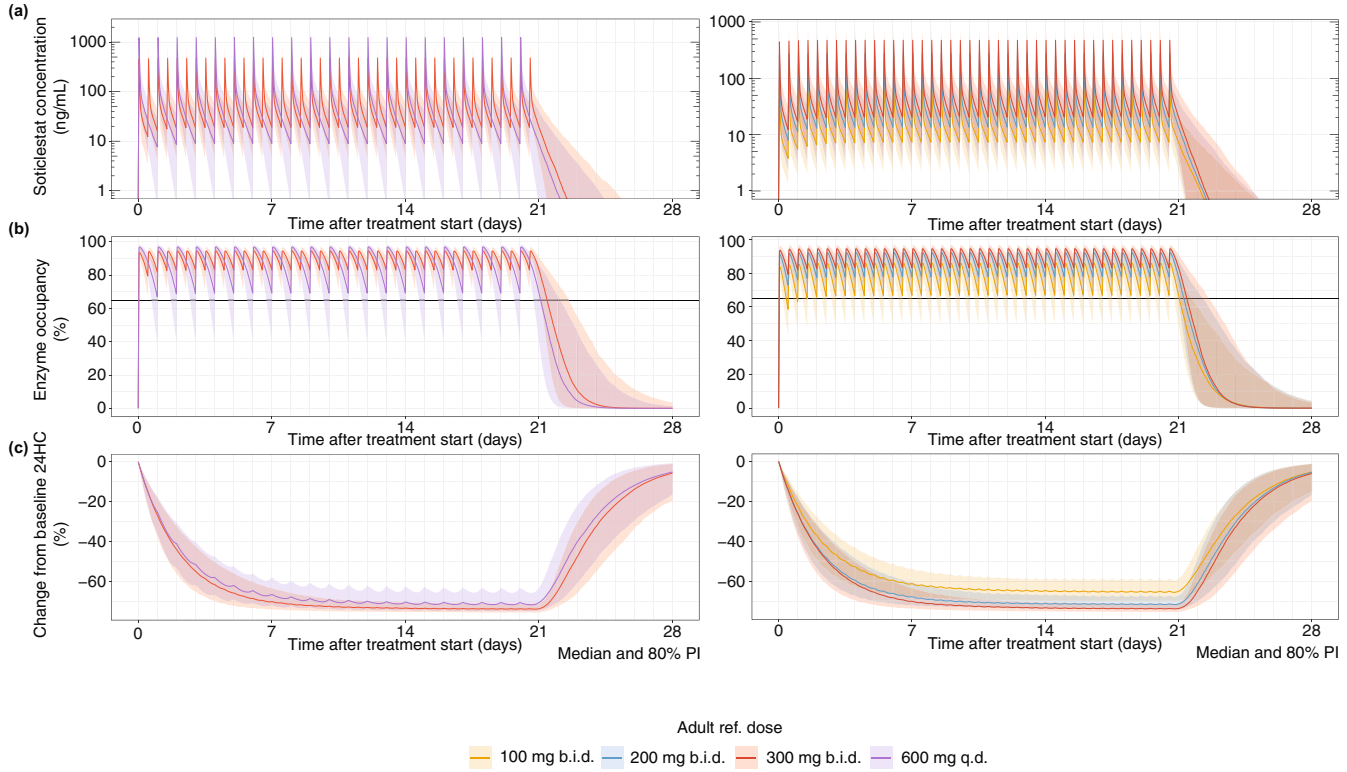

FIGURE 4 Model-based simulations of various soticlestat dosing regimens. Soticlestat concentrations (ng/ml) (a), enzyme occupancy (%) (b), and change from baseline 24HC (%) (c) over 21 days with 7-day washout. Solid lines: median; shaded area: 80% PI. 24HC, 24*S*-hydroxycholesterol; b.i.d., twice daily; PI, prediction interval; q.d., once daily: ref., reference.

was reduced from 240 mg to 220 mg (administered b.i.d.) and, for the 15–19 kg weight group, from 280 mg to 260 mg (administered b.i.d.). The projected CH24H occupancy at steady-state in the brain was above the target EO value of 65% for all doses (Figure 5). The resulting pediatric median exposure was predicted to be within 30% of the adult reference exposure in all weight groups. Table S4 lists the final recommended daily doses for children and adolescents weighing 10–100 kg (split into 11 weight groups).

DISCUSSION

This report describes the successful development of a population mixed-effect model to characterize the PK and PK/PD relationship of soticlestat in healthy adults, along with exploration and prediction of CH24H occupancy as a measure of target engagement. Simulations based on the final model were used to inform decisions about phase II clinical trial design, including dose selection in studies of pediatric and adult patients with DEEs.[4,7] The use of a model-informed approach to generate these results demonstrates the valuable role of quantitative techniques in optimizing clinical study design and improving accuracy of dose selection, particularly for populations with rare pediatric conditions, such as DS and LGS.[4,6,7]

The PopPK model adequately described the soticlestat PK data from all four included phase I studies and contained transit and absorption compartments to account for the delay in absorption for the tablet formulation. Dose was included as a covariate on CL/F, Q/F, and V_p/F based on visual evaluation of goodness of fit plots and the concentration versus time profile plots for soticlestat at different dose levels. The exact mechanism of apparent slight nonlinearity in the PK profile of soticlestat was not mechanistically evaluated at this time, however, the empirical approach used here was sufficient to develop a model that accurately represented the observed concentration versus time profile data for soticlestat. Furthermore, the predicted soticlestat exposures based on model-informed simulations from the current study were consistent with observed exposures in subsequent pediatric clinical trials that utilized the weight-adjusted pediatric doses recommended from this study.[7] Therefore, the assumed similarity of nonlinearity across populations was reasonable in the absence of data and the empirical approach used during this analysis was sufficient to provide adequate dose recommendation for pediatric populations. The PK/EO model captured the relationship between soticlestat concentrations and CH24H occupancy, and accounted for the delay and observed hysteresis in plasma soticlestat concentrations and brain occupancy by appropriately

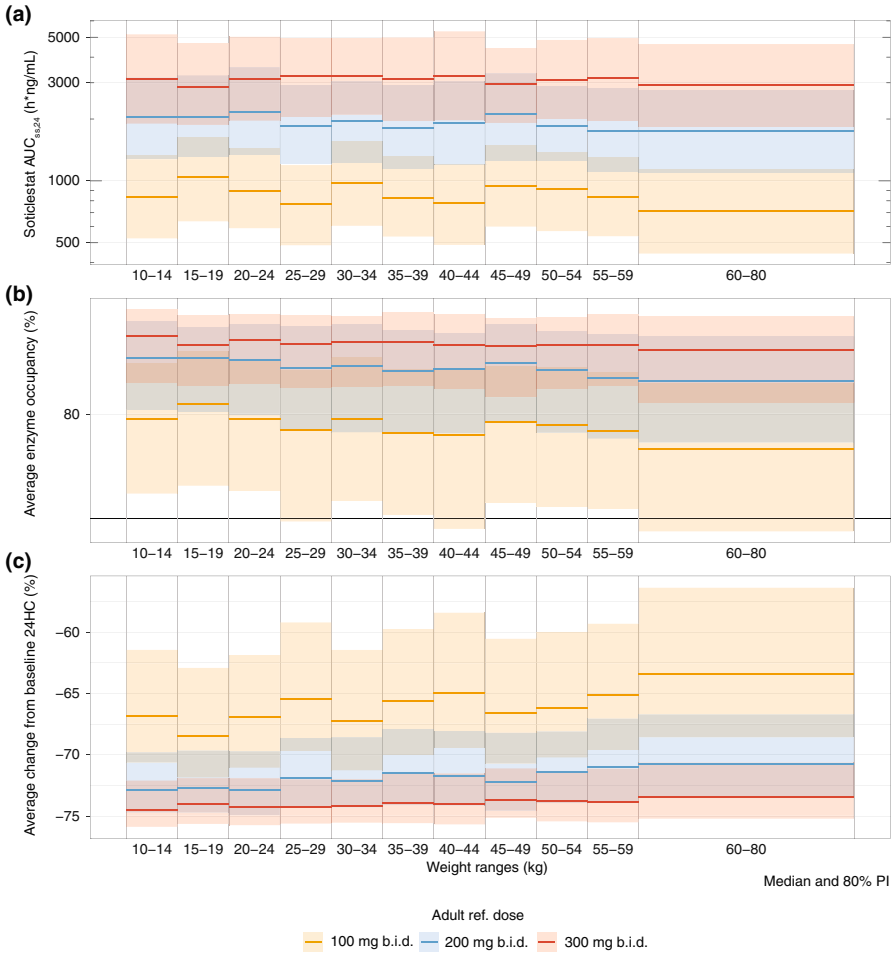

FIGURE 5 Simulated exposure, EO, and change from baseline 24HC utilizing proposed weight-based dosing. (a) AUC soticlestat: $AUC_{ss,24}$ (ng*mL/h), with low (yellow), middle (blue), or high (red) dosage, equivalent to 100 mg b.i.d., 200 mg b.i.d., or 300 mg b.i.d. soticlestat for a 70 kg reference patient, (b) EO: EO with low (yellow), middle (blue), or high (red) dosage, equivalent to 100 mg b.i.d., 200 mg b.i.d., or 300 mg b.i.d. soticlestat for a 70 kg reference patient (solid gray line is 65% target EO), (c) 24HC: change from baseline 24HC with low (yellow), middle (blue), or high (red) dosage, equivalent to 100 mg b.i.d., 200 mg b.i.d., or 300 mg b.i.d. soticlestat for a 70 kg reference patient. Solid line: median; shaded area: 80% PI. 24HC, 24*S*-hydroxycholesterol; AUC, area under the plasma concentration–time curve; $AUC_{ss,24}$, median area under the plasma concentration–time curve at steady-state over 24 h; b.i.d., twice daily; EO, enzyme occupancy; PI, prediction interval; ref., reference.

implementing an effect-site compartment. The inhibitory indirect response PK/PD model described the relationship between soticlestat and 24HC concentrations well, and the final PK/EO/PD model was suitable for simulating the effect of different dosing regimens on 24HC. Very good model parameter precision was observed and there was no marked departure on GOF or visual predictive check plots, with adequate description of central tendency and variability in the observed data.

Clinical trial simulations suggested that b.i.d. dosing of soticlestat was preferable to q.d. dosing to achieve target CH24H occupancy and reduce fluctuations during the dosing interval. Additionally, soticlestat 100–300 mg b.i.d. dosing was associated with desired CH24H occupancy and reductions in plasma 24HC concentrations from baseline for an adult weighing 60 kg or more. All examined b.i.d. doses achieved CH24H occupancy over the target of 65%. Based on being associated with the highest CH24H occupancy levels and therefore potentially the greatest efficacy, 300 mg b.i.d. was selected as the preferred dosage to examine in phase II studies. When needed, patients unable to tolerate 300 mg b.i.d. could receive 200 mg b.i.d., which would still achieve target CH24H occupancy based on the simulations.

Together, these findings informed the design of a phase Ib/IIa clinical trial evaluating the safety and tolerability of soticlestat as an adjunctive therapy in 18 adults with DEEs.[4] The study included a randomized, placebo-controlled period that assessed soticlestat titrated up to a final target dosage of 300 mg b.i.d. over a 30-day period, followed by a 60-day open-label period. PK/PD parameters were similar to those modeled in the present analysis (e.g., clearance

was 190–259.4 L/h vs. 204 L/h in the present analysis, and mean percent change from baseline in plasma 24HC was −76.88% at day 21 vs. −73.4% in the present analysis). Soticlestat was well-tolerated, with 71.4% of participants receiving soticlestat and 100% of participants receiving placebo experiencing at least one treatment-emergent adverse event (TEAE). In the open-label period, 68.8% of participants experienced at least one TEAE. Median percentage reduction from baseline seizure frequency in the open-label maintenance phase period was 36.4%.[4]

Further simulations allowed progression from phase I studies in healthy adults to phase II studies in the target pediatric patient population with DS or LGS. Appropriate doses were identified for children and adolescents weighing 10–60 kg, with adjustments being made for children weighing 10–20 kg to avoid overexposure. These dosing strategies were utilized in the ELEKTRA study (NCT03650452), which examined efficacy and safety of soticlestat in children with DS or LGS.[7] Findings from ELEKTRA supported the validity of the PK/EO/PD model. TEAE incidences were similar between the soticlestat (80.3%) and placebo (74.3%) groups, with 5% of patients ($n = 7$) withdrawing from the study owing to TEAEs (soticlestat, $n = 4$, [5.6%]; placebo, $n = 3$ [4.3%]). For the primary end point of frequency of convulsive seizures (for DS) and drop seizures (for LGS) in the combined patient population in the maintenance period, patients receiving soticlestat demonstrated a statistically significant median placebo-adjusted reduction in seizure frequency of 30.5% ($p = 0.0007$). The PK and PD profiles observed in ELEKTRA were consistent with the model-based simulations described in the present analysis.[7]

Modeling and simulating PK, EO, and PD in various scenarios facilitates optimal dose selection and design of subsequent clinical trials, thereby guiding conduct of pediatric trials, despite limited safety and efficacy data in the adult patient population. Additionally, rapid acceleration of pediatric drug development is enabled by increasing precision and confidence in dose selection for populations with rare conditions. MIDD thus aids efficient clinical trial design and achievement of adequate statistical power, even with limited patient numbers. Clinical trial simulations also allow uncertainty about dose selection and other factors to be quantified, which can optimize detection of efficacy in clinical trials by informing the required sample size and demonstrating the feasibility of further clinical development.[7]

MIDD is particularly important in conditions affecting children, given the differences between adults and children in body composition, physiology, and biochemistry that may alter dosing requirements.[6] Furthermore, for rare diseases, such as DS and LGS,[7] the patient population is limited by definition and few patients are available for clinical trials. To this end, MIDD can provide crucial evidence to support dosing strategies, which can reduce or eliminate the need for clinical trials. In the case of adalimumab, the U.S. Food and Drug Administration approval for adolescent patients with hidradenitis suppurativa was granted solely on the basis of PK modeling of data from affected adults and pediatric patients with other diseases.[6]

Limitations of this study include the assumptions made in the analyses; for example, assumptions made when simulating pediatric data based on a model developed for an adult population. The extensive modeling undertaken to avoid overexposure and the positive safety and efficacy results obtained thus far provide confidence in these model-based simulations.[7] However, the developed model is only applicable to children older than 2 years of age. Subsequent model development will include a maturation factor to allow simulations for children younger than 2 years of age.

Strengths of the present analysis include the use of data from four different studies, which facilitated examination of PK/EO/PD data across a range of scenarios (e.g., in terms of dose amount and q.d. vs. b.i.d. dosing).

In conclusion, the developed PK/EO/PD model fitted the observed data well and successfully informed the design of a phase Ib/IIa study to assess the safety and tolerability of soticlestat in adults with DEEs, as well as a phase II study investigating the efficacy and safety of soticlestat in children with DEEs. In these pediatric studies, soticlestat was well-tolerated and efficacy results were promising, confirming the appropriateness of the selected dosing regimens.

AUTHOR CONTRIBUTIONS

All authors were involved in designing the research, performing the research, analyzing the data, and writing the manuscript.

ACKNOWLEDGMENTS

All studies were funded by the sponsor, Takeda Pharmaceutical Company Ltd. Under the direction of the authors and funded by Takeda Pharmaceutical Company Ltd, Dr A.L. Jones and Dr E. Butcher of Oxford PharmaGenesis, Oxford, UK, provided writing assistance for this publication. Editorial assistance in formatting, proofreading, copyediting, and fact checking was also provided by Oxford PharmaGenesis. The contents of this manuscript, the interpretation of the data, and the decision to submit the manuscript for publication in *Clinical and Translational Science* were made by the authors independently.

FUNDING INFORMATION

All studies included in this manuscript were funded by the sponsor, Takeda Pharmaceutical Company Ltd.

CONFLICT OF INTEREST STATEMENT

W.Y., M.A., and M.V. are employees of Takeda Pharmaceutical Company Ltd and own stock or stock options. A.F., T.W., and G.L. are former employees of Takeda and received payment for acting as consultants for Takeda at the time of data analysis. M.T. is a former employee of Takeda and was employed by Takeda at the time of data analysis.

DATA AVAILABILITY STATEMENT

The datasets, including the redacted study protocol, redacted statistical analysis plan, and individual participants data supporting the results reported in this article, will be available 3 months after the submission of a request, to researchers who provide a methodologically sound proposal. The data will be provided after its de-identification, in compliance with applicable privacy laws, data protection, and requirements for consent and anonymization.

ORCID

Wei Yin https://orcid.org/0000-0002-4834-5783

REFERENCES

1. Nishi T, Kondo S, Miyamoto M, et al. Soticlestat, a novel cholesterol 24-hydroxylase inhibitor shows a therapeutic potential for neural hyperexcitation in mice. *Sci Rep*. 2020;10:17081.
2. Paul SM, Doherty JJ, Robichaud AJ, et al. The major brain cholesterol metabolite 24(S)-hydroxycholesterol is a potent allosteric modulator of N-methyl-D-aspartate receptors. *J Neurosci*. 2013;33:17290-17300.
3. Nury T, Zarrouk A, Mackrill JJ, et al. Induction of oxiapoptophagy on 158N murine oligodendrocytes treated by 7-ketocholesterol-, 7beta-hydroxycholesterol-, or 24(S)-hydroxycholesterol: protective effects of alpha-tocopherol and docosahexaenoic acid (DHA; C22:6 n-3). *Steroids*. 2015;99:194-203.
4. Halford JJ, Sperling MR, Arkilo D, et al. A phase 1b/2a study of soticlestat as adjunctive therapy in participants with developmental and/or epileptic encephalopathies. *Epilepsy Res*. 2021;174:106646.
5. Benarroch EE. Brain cholesterol metabolism and neurologic disease. *Neurology*. 2008;71:1368-1373.
6. Bi Y, Liu J, Li F, et al. Model-informed drug development in pediatric dose selection. *J Clin Pharmacol*. 2021;61(Suppl 1):S60-S69.
7. Hahn CD, Jiang Y, Villanueva V, et al. A phase 2, randomized, double-blind, placebo-controlled study to evaluate the efficacy and safety of soticlestat as adjunctive therapy in pediatric patients with Dravet syndrome or Lennox–Gastaut syndrome (ELEKTRA). *Epilepsia*. 2022;63:2671-2683.
8. Koike T, Yoshikawa M, Ando HK, et al. Discovery of soticlestat, a potent and selective inhibitor for cholesterol 24-hydroxylase (CH24H). *J Med Chem*. 2021;64:12228-12244.
9. Koike T, Constantinescu CC, Ikeda S, et al. Preclinical characterization of [18F] T-008, a novel PET imaging radioligand for cholesterol 24-hydroxylase. *Eur J Nucl Med Mol Imaging*. 2022;49:1148-1156.
10. Nishi T, Metcalf CS, Fujimoto S, et al. Anticonvulsive properties of soticlestat, a novel cholesterol 24-hydroxylase inhibitor. *Epilepsia*. 2022;63:1580-1590.
11. Wang S, Chen G, Merlo Pich E, Affinito J, Cwik M, Faessel H. Safety, tolerability, pharmacokinetics, pharmacodynamics, bioavailability and food effect of single doses of soticlestat in healthy subjects. *Br J Clin Pharmacol*. 2021;87:4354-4365.
12. Wang S, Chen G, Merlo Pich E, Affinito J, Cwik M, Faessel HM. Pharmacokinetics, pharmacodynamics and safety assessment of multiple doses of soticlestat in healthy volunteers. *Br J Clin Pharmacol*. 2022;88:2899-2908.
13. Takeda. A phase 1 positron emission tomography study to measure cholesterol 24S-hydroxylase target occupancy of TAK-935. 2017 Accessed February 3, 2022.
14. Tauscher J, Tauscher J, Cole PE, Brown T, et al. A PET study with [18F]MNI-792 to determine cholesterol 24S-hydroxylase occupancy of TAK-935 in healthy subjects. *J. Cereb. Blood Flow Metab.* 2019;39:524-608. PP501-M506.
15. Asgharnejad M, Yin W, Ballard TE, et al. Absolute bioavailability and mass balance of the CH24H inhibitor soticlestat in healthy volunteers [poster]. Presented at the American Epilepsy Society Annual Meeting 2022, 2–6 December 2022, Nashville, TN, USA.
16. Centers for Disease Control and Prevention. Clinical Growth Charts. 2000 (last updated June 16, 2017); Accessed Aug 24, 2022.

SUPPORTING INFORMATION

Additional supporting information can be found online in the Supporting Information section at the end of this article.

How to cite this article: Yin W, Facius A, Wagner T, et al. Population pharmacokinetics, enzyme occupancy, and 24*S*-hydroxycholesterol modeling of soticlestat, a novel cholesterol 24-hydroxylase inhibitor, in healthy adults. *Clin Transl Sci*. 2023;16:1149-1162. doi:10.1111/cts.13517